



Highly selective metal fluoride catalysts for the dehydrohalogenation of 3-chloro-1,1,1,3-tetrafluorobutane

Katharina Teinz^a, Stefan Wuttke^{a,b}, Fabian Börno^a, Johannes Eicher^c, Erhard Kemnitz^{a,*}

^a Institut für Chemie, Humboldt-Universität zu Berlin, Brook-Taylor-Straße 2, 12489 Berlin, Germany

^b Department of Chemistry and Center for NanoScience (CeNS), University of Munich (LMU), Butenandtstraße 11, 81377 München, Germany

^c Solvay Fluor GmbH, Hans-Böckler-Allee 20, 30173 Hannover, Germany

ARTICLE INFO

Article history:

Received 29 March 2011

Revised 6 June 2011

Accepted 12 June 2011

Available online 16 July 2011

Keywords:

Dehydrochlorination

Dehydrofluorination

Heterogeneous catalysis

Nanoscopic metal fluorides

Sol–gel synthesis

Lewis acid

Lewis base

ABSTRACT

For the first time, dehydrochlorination and dehydrofluorination reactions are studied on the same substrate, 3-chloro-1,1,1,3-tetrafluorobutane, employing nanoscopic metal fluorides AlF_3 , MgF_2 , CaF_2 , SrF_2 , and BaF_2 as catalysts that are prepared according the *fluorolytic* sol–gel synthesis. AlF_3 is exclusively selective toward dehydrofluorination, whereas BaF_2 is 100% selective toward dehydrochlorination. The acid–base character of the catalysts is investigated and, as a result, mechanistic proposals for the dehydrofluorination and the dehydrochlorination are given. Thus, at high conversion level, selective catalysts for both dehydrofluorination and dehydrochlorination on the same substrate have been developed.

© 2011 Elsevier Inc. All rights reserved.

1. Introduction

The goal of research in catalysis is currently accompanied by the development of many different methods of preparing catalysts in an attempt to optimize their properties. The aim is to develop a catalyst that exhibits 100% selectivity for a desired product by 100% conversion of the reaction, thus preventing by-product formation and eliminating waste. By doing so, on the one side, an understanding of the already used catalysts is necessary, but on the other side, new synthesis routes for catalysts must be developed.

In 2003, our group explored the *fluorolytic* sol–gel synthesis for the preparation of metal fluorides for the first time [1]. This synthesis starts with metal alkoxides and nonaqueous [2] (or aqueous) HF [3] followed by the gas-phase fluorination of the obtained dry gel with mild fluorination agents. This yields high surface area metal fluorides that have different properties in comparison with conventionally prepared fluorides [4]. An advantage of these new metal fluorides are their tunable surface properties with consequences for catalytic applications. These new materials were already successfully used as heterogeneous catalysts possessing high activity as well as a high selectivity in the synthesis of (all-

rac)- α -tocopherol (vitamin E) [5,6], the one-pot synthesis of menthol [7,8] and vitamin K_1 as well as K_1 -chromanol [9]. However, all these examples are either purely acid catalyzed or bi-functionalized with gold that catalyzes a hydrogenation step.

In this report, we focus on the acid–base pair properties of the metal fluorides and the consequences for dehydrohalogenation reactions. For this purpose, aluminum fluoride and alkaline earth metal fluorides (MgF_2 , CaF_2 , SrF_2 , and BaF_2) were synthesized according to the *fluorolytic* sol–gel synthesis. It is expected that Lewis acidity decreases from AlF_3 to BaF_2 due to the increase in the ionic radius and the decrease in the positive charge density. At the same time, the Lewis basicity should increase. The goal is to investigate these properties and to relate acid–base with catalytic properties. The metal fluorides were tested for the dehydrohalogenation of the chlorofluoroalkane, 3-chloro-1,1,1,3-tetrafluorobutane, where either dehydrochlorination or dehydrofluorination can take place.

Haloalkenes are very important starting compounds for halogen-containing polymers (e.g. PVC, PVdC, PVDF, and PTFE). Because of the easy access to a huge variety of haloalkanes, they are an interesting source for haloalkenes production. The general approach toward haloalkenes starting from haloalkanes is either a dehydrochlorination or a dehydrofluorination reaction. In both cases, heterogeneous catalysts are required for a green chemical synthesis.

* Corresponding author. Fax: +49 3020937277.

E-mail address: erhard.kemnitz@chemie.hu-berlin.de (E. Kemnitz).

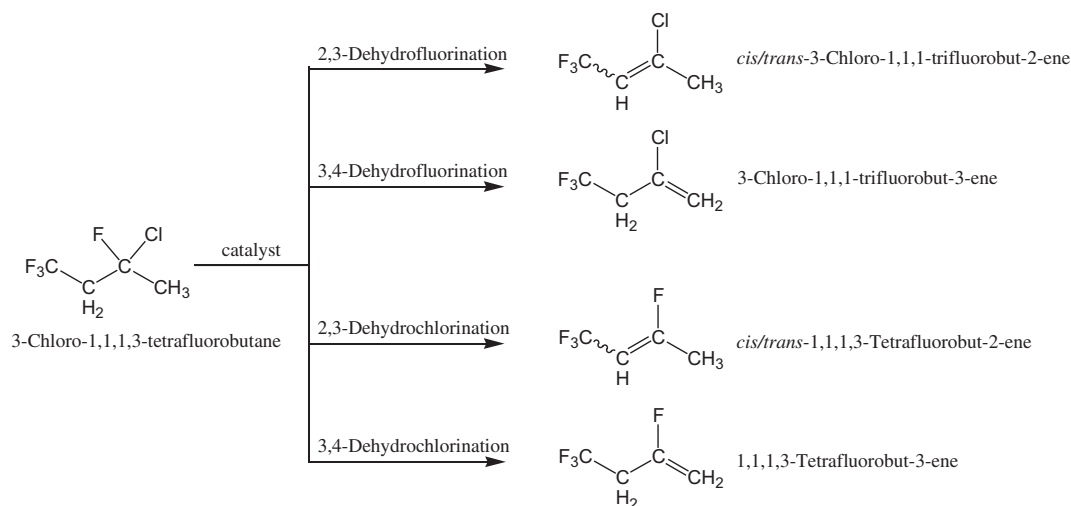


Fig. 1. Reaction scheme for the dehydrohalogenation of 3-chloro-1,1,1,3-tetrafluorobutane.

For dehydrochlorination of chloroalkanes, only a few important papers were published within the past decade. Mishakov et al. found that nano-crystalline magnesium oxide is partly converted into magnesium chloride during its reaction with 1-chlorobutane (conversion rate: $0.004 \mu\text{mol s}^{-1} \text{m}^{-2}$ at 200°C), which gives the alkene [10]. Furthermore, Pistarino et al. used silica–alumina substrate to dehydrochlorinate 1,2-dichloropropane [11]. Kamiguchi et al. used Nb-, Mo-, Ta-, W-, and Re-halogenide clusters for the dehydrochlorination of 1-chloro- and 2-chloropentane and dehydrofluorination of 1-fluoropentane [12]. To the best of our knowledge, no systematic studies have been performed so far concerning the dehydrohalogenation of a chlorofluoroalkane where both, dehydrochlorination and dehydrofluorination, are investigated on the same substrate. Therefore, by applying different nanoscopic metal fluorides as catalysts with tuned acid–base properties at their surfaces, it was the intention of this investigation to understand the role of the catalytic surface sites. Thus, based on gained mechanistic insights, fine tuning of the acid–base properties and optimized selectivity toward either of the dehydrohalogenation reactions was anticipated.

Lewis acids are known to activate C–X bonds, which is the initial step of a dehydrohalogenation reaction. Thermodynamically, C–F bond activation is less probable than C–Cl bond activation. That is why only very strong Lewis acids should be active for dehydrofluorination whereas dehydrochlorination should be catalyzed by far more Lewis acidic catalysts.

As a chlorofluorocarbon target molecule we chose 3-chloro-1,1,1,3-tetrafluorobutane since this is an industrially interesting and promising substrate resulting in valuable haloalkenes after HX elimination. In Fig. 1, the reaction scheme is shown. Three different dehydrochlorination and another three different dehydrofluorination products might be formed this way. If these two dehydrohalogenation reactions become catalyzed, further consecutive reactions with the formed HX have to be considered, which would result in two further possible side products, namely 1,1,1,3-pentafluorobutane and 3,3-dichloro-1,1,1-trifluorobutane.

2. Experimental

2.1. Fluorolytic sol–gel synthesis

In course of the present investigations, the *fluorolytic* sol–gel synthesis was for the first time also applied to strontium fluoride. The syntheses of the other fluorides are already described in the literature [13].

Hydrogen fluoride (Solvay Fluor GmbH), sodium hydrogen carbonate (Roth, >99.5%), aluminum isopropoxide (Aldrich, >98%), magnesium ethoxide (Aldrich, 98%), calcium methoxide (Aldrich, 97%), strontium (Aldrich, granular 99%), and barium (Aldrich, rods 99+%) were used as received. Methanol (Aldrich, 99%), isopropanol (Aldrich, 99%), and tetrahydrofuran (Aldrich, 99%) were dried according to the standard procedure before use. All operations were carried out under inert conditions.

The methoxides of strontium and barium were prepared through the reaction of the respective metal with methanol excess. For the *fluorolytic* sol–gel synthesis, metal alkoxides were dissolved or suspended in isopropanol (aluminum fluoride), tetrahydrofuran (magnesium fluoride), or methanol (calcium, strontium, and barium fluoride), which was followed by the addition of a stoichiometric amount of hydrogen fluoride dissolved in methanol. Caution: HF is dangerous and must be handled with the appropriate precautions. After fifteen hours, dry xerogels were obtained by evaporating the solvents from the wet gel under vacuum ($\sim 5 \times 10^{-3}$ mbar) and further drying at 100°C for 2 h.

The “BaF₂ left at air” used for catalysis is a BaF₂ xerogel that after preparation was grinded at air.

2.2. Catalytic reactions

A quartz tube (inner diameter 8 mm) with a stopper of quartz wool was used as steady flow reactor. 3-chloro-1,1,1,3-tetrafluorobutane (Solvay Fluor GmbH, 84% 3-chloro-1,1,1,3-tetrafluorobutane, 7% 3-chloro-1,1,1-trifluorobut-3-ene, 2% 3-chloro-1,1,1-trifluorobut-2-ene, 2% 1,1,1,3,3-pentafluorobutane, and 5% other impurities) was dosed via a gas saturator using nitrogen as carrier gas (nitrogen flow: 20 ml min^{-1} , total flow: 25 ml min^{-1}). If not mentioned otherwise, the contact time was kept for 0.5 s (200–300 mg of xerogel, dumping height: 0.4 cm) and the reaction temperature at 200°C . The reaction gas mixture leaving the reactor was passed through a 0.5 M sodium hydrogen carbonate solution to trap acid gases. An analysis of the reaction mixture was performed by gas chromatography by injecting a sample of 250 μl into a Shimadzu GC 17A equipped with a PONA column (50 m \times 0.2 mm \times 0.5 μm), considering the impurities.

2.3. Catalyst characterization

X-ray powder diffraction measurements were performed using a Seifert XRD3003TT diffractometer using Cu K α radiation. Moisture sensitive samples were prepared in a glove box and covered

with a Kapton foil. The solids used for catalysis were identified based on the ICSD powder diffraction file [14].

The chlorine content of the catalysts was determined by the titration of the nitric acid neutralized alkaline pulping solution with 0.01 N mercury perchlorate solution with diphenylcarbazone as an indicator.

Surface area measurements were performed on a Micromeritics ASAP 2020 at 77 K by nitrogen adsorption. Before the measurement, the solids were degassed at 120 °C and 5×10^{-5} mbar for twelve hours. Isotherms were processed by the Brunauer–Emmett–Teller method (BET).

For FT-IR photoacoustic spectroscopy with ammonia as probe molecule (NH₃-PAS), an MTEC 300 photoacoustic cell inside a Digilab Excalibur FTS 300 spectrometer was used. Before the measurement, the solids were preheated at 150 °C in a nitrogen flow, loaded with ammonia, and purged with nitrogen.

The temperature-programmed desorption profiles of ammonia (NH₃-TPD) were recorded with a Perkin Elmer FTIR-System 2000 at 930 cm⁻¹. The preheated (200 °C) solid was loaded with ammonia at 120 °C. After purging with nitrogen (10 ml min⁻¹, 30 min), the temperature was raised by 10 K min⁻¹ until reaching 500 °C while the desorbed ammonia was recorded.

IR spectra were recorded on a Nicolet Magna 550 spectrometer equipped with a liquid nitrogen cooled MCT detector in transmission mode and purged by a dry nitrogen flow. The resolution was 4 cm⁻¹ and 128 scans were co-added for each spectrum, in a transmission range of 1000–4000 cm⁻¹. The cell for IR analysis consisted of vitreous silica and was equipped with CaF₂ windows. A moveable quartz sample holder permits the adjustment of the pellet in the infrared beam for acquisition of spectra and its displacement into a furnace at the top of the cell for thermal treatments. The cell was connected to a vacuum line and a glass injection loop with a known volume (2.15 cm³). The sample was pressed into a self-supporting pellet (area, 2 cm²; pressure, 1.5 tons; mass, 10–20 mg) in air or in a dry glove box. After connecting the IR cell to the vacuum line, the sample was heated at 473 K for 12 h. After the activation of the sample, different probe molecules were added in small doses.

3. Results

3.1. Catalyst characterization

If not mentioned, otherwise the characterization of the solids was done after catalytic runs over two hours.

3.1.1. XRD patterns

In Fig. 2, XRD patterns of the studied fluorides are shown. Aluminum fluoride is X-ray amorphous. The alkaline earth metal fluorides show broad reflexes and the maxima of diffractograms correspond to the crystalline fluorides (see PDF card numbers in figure caption). With the aid of Debye–Scherrer equation, a crystallite size of about 10 nm was estimated. XRD patterns of barium fluoride after catalysis do not show reflexes for BaF₂ as the xerogel (inert as well as exposed to air), but they can be assigned to BaClF. Obviously, a chlorination of the BaF₂ xerogel occurs during the reaction with 3-chloro-1,1,1,3-tetrafluorobutane. This chlorofluoride phase is observed even after 20 h of reaction time, which indicates its stability under the reaction conditions. Moreover, no indications for BaCl₂ formation were found.

3.1.2. Chlorine content

In Table 1, chlorine contents of the used catalysts are shown. Only for strontium fluoride as well as barium fluoride, chlorine could be detected after the reaction. The chlorine content of the

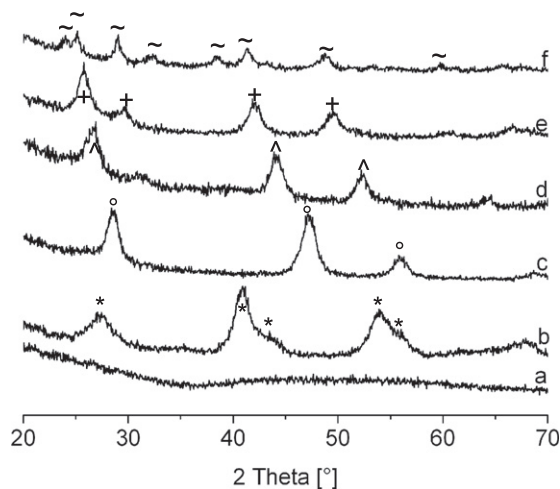


Fig. 2. XRD patterns of catalysts after reaction: AlF₃ (a), MgF₂ (b, * PDF 1-1196), CaF₂ (c, ° PDF 3-1088), SrF₂ (d, ^ PDF 88-2294), BaF₂ (f, ~ PDF 3-304) and xerogel BaF₂ (e, + PDF 1-533).

barium fluoride that was left in air was significantly higher in comparison with the barium fluoride which was handled under inert conditions. After four hours of reaction time, the maximum of chlorine content was reached and remained constant over at least six-teen additional hours of reaction. Based on these data, for the catalytic active phase of in-air handled barium fluoride was calculated a total formula of BaCl_{0.7}F_{1.3}.

3.1.3. Surface area

As shown in Table 2, the used fluorides provide different surface areas. The main reason for these differences is due to the different crystallization temperature of the xerogels. It was found that the crystallization of nanoscopic MgF₂ depends on the gas-phase composition at around 250 °C whereas AlF₃ crystallizes above 300 °C [15,16]. The quite diverse surface areas of the barium fluorides can be rationalized by their different chemical composition. The inert handled BaF₂ represents BaCl_{0.3}F_{1.7}, whereas BaF₂ air corresponds to BaCl_{0.5}F_{1.5} (Section 3.1.2) during catalysis.

3.1.4. Acidity: NH₃-PAS and NH₃-TPD

With NH₃-PAS, strong Lewis acidic sites (1340 cm⁻¹) and medium Brønsted acidic (1430 cm⁻¹) sites were found for aluminum fluoride. Calcium fluoride and strontium fluoride show only Brønsted acidic sites (1450 cm⁻¹). The occurrence of Brønsted acidic sites is caused by the adsorption of hydrogen fluoride on Lewis acidic sites during the catalytic reaction [17]. In the case of aluminum fluoride, the adsorption of hydrogen fluoride was also proven by MAS NMR (not shown here). Unfortunately, NH₃-PAS is not sensitive enough to find any acidic sites on magnesium fluoride and barium fluoride – although we have already shown medium Lewis acidity for magnesium fluoride probed with CO [18].

The NH₃-TPD profiles for all of the studied fluorides are shown in Fig. 3. For aluminum fluoride, an intense profile is found with two maxima at ~200 °C and ~400 °C evidencing the presence of strong acid sites [1]. For magnesium fluoride, calcium fluoride, and strontium fluoride, ammonia desorption is already completed at 300 °C due to medium acidic sites. Barium fluoride did not adsorb any detectable amounts of ammonia.

3.1.5. Acidity: Adsorption of CO on different BaF₂-samples

CO is a suitable probe molecule for the characterization of Lewis acidity because the ν(CO) frequency is very sensitive to the local cationic environment [19]. The wave number of the linear ν(CO)

Table 1
Chlorine content of catalysts after reaction.

Catalysts	Reaction time (h)	Chlorine content (wt.%)	Chemical composition
AlF ₃	2	–	–
MgF ₂	2	–	–
CaF ₂	2	–	–
SrF ₂	2	4	SrCl _{0.1} F _{1.9}
BaF ₂	2	6	BaCl _{0.3} F _{1.7}
BaF ₂ air	2	10	BaCl _{0.5} F _{1.5}
BaF ₂ air	4	13	BaCl _{0.7} F _{1.3}
BaF ₂ air	20	13	BaCl _{0.7} F _{1.3}

Table 2
Surface area of catalysts after reaction determined by the BET model.

Catalysts	Surface area (m ² g ⁻¹)
AlF ₃	220
MgF ₂	40
CaF ₂	250
SrF ₂	40
BaF ₂	20
BaF ₂ air	60

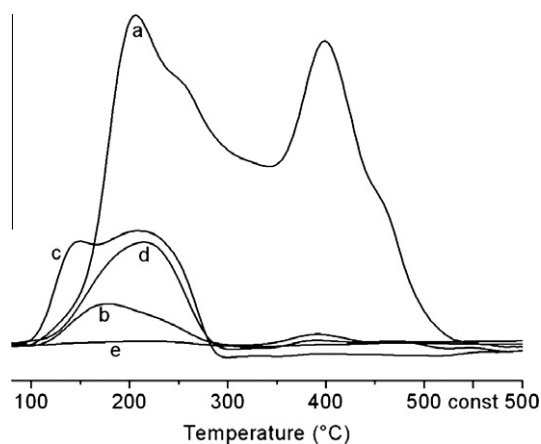


Fig. 3. NH₃-TPD profiles of catalysts after reaction: AlF₃ (a), MgF₂ (b), CaF₂ (c), SrF₂ (d), BaF₂ (e).

stretching vibration of molecules, adsorbed at Lewis acidic centers without electronic back-donation, is shifted to higher wave numbers than in gaseous CO ($\nu_{\text{gas}} = 2143 \text{ cm}^{-1}$). Thus, the higher the blue shift, the higher the Lewis acidity. As it was already shown with CO, AlF₃ possesses very strong Lewis acidity [20], whereas MgF₂ shows acid centers with medium strength [18]. Therefore, we investigated here the different BaF₂ samples in more detail in order to compare all these samples and to better understand the catalytic results below.

All BaF₂ samples (BaF₂, BaF₂ air, and BaCl_{0.7}F_{1.3}) show the same bands after CO adsorption. Fig. 4 presents the spectra of BaCl_{0.7}F_{1.3} recorded after adsorption of small doses of CO at 100 K. The first dose displays a band at 2166 cm⁻¹ that slightly shifted at higher CO coverage. After the adsorption of 1 Torr of CO at equilibrium pressure, the band is observed at 2162 cm⁻¹. Since no perturbation occurs in the $\nu(\text{OH})$ range (not shown), this band can be assigned to CO adsorbed on coordinatively unsaturated Ba²⁺ sites. Moreover, the shoulder at lowest frequency (around 2154 cm⁻¹) only develops at high partial pressures and this is typical of weak and unspecific adsorption of CO. The unusually low frequency of the $\nu(\text{CO})$ band on the unsaturated Ba²⁺ sites is in agreement with the result

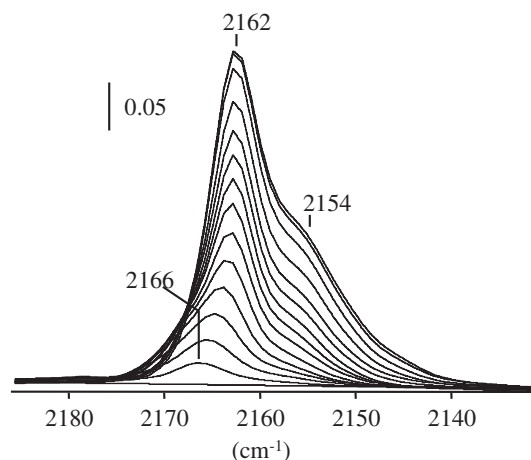


Fig. 4. CO stretching region of the IR spectra of adsorbed CO on BaCl_{0.7}F_{1.3} outgassed at 473 K and after adding successive doses of CO at 100 K and finally 1 Torr of CO at equilibrium pressure.

of adsorbed CO on barium cations in zeolites [21] and on BaO/ZrO₂ [22]. Hence, all the BaF₂ samples possess very weak Lewis acid sites.

3.1.6. Basicity: Adsorption of CHCl₃ and pyrrole on the different BaF₂-samples

By using CHCl₃ and pyrrole as probe molecules [18], we have detected the basicity of a solid fluoride material for the first time. For the prepared sol-gel MgF₂, some Lewis basicity is observed, but at the same time, the Lewis acid centers are the dominating sites in the acid–base pair when a probe molecule is adsorbed. However, by increasing the ionic radius with constant charge (from MgF₂ to BaF₂), a decrease in the Lewis acidity as well as an increase in the Lewis basicity is expected.

CHCl₃ fulfills the criteria for interacting separately with either a Lewis acid site or a base site or simultaneously with both sites [23,24]. Therefore, it can be predicted which of the acid–base pair reaction is playing the key role during a catalytic process. CHCl₃ adsorption reveals that all BaF₂ samples (BaF₂, BaF₂ air, and BaCl_{0.7}F_{1.3}) display the same bands and consequently the same interactions occur with this probe molecule. Fig. 5 presents the spectra for BaCl_{0.7}F_{1.3}, which is recorded after the introduction of 1 Torr of CHCl₃ at equilibrium pressure (Fig. 5a). This is followed by a progressive evacuation at room temperature (Fig. 5b–f). After the adsorption of 1 Torr of CHCl₃ at equilibrium pressure, the spectra display a broad band at 3009 cm⁻¹ as well as a small band at 3033 cm⁻¹. The blue shift of the $\nu(\text{CH})$ band ($\nu_{\text{gas}} = 3019 \text{ cm}^{-1}$) [23] at 3033 cm⁻¹ indicates an interaction of the lone pair of a chlorine atom of the chloroform molecule with a Lewis acid site ($\text{M}^{\text{x}+} \leftarrow \text{Cl}-\text{CHCl}_2$). However, this interaction lowers the symmetry of CHCl₃ from C_{2v} for the isolated molecule to the C_s point group. This leads to a splitting of the ν_4 band ($\nu_{\text{gas}} = 2116 \text{ cm}^{-1}$) [23], which could not be observed (Fig. 5). This result suggests that this interaction is very weak and plays an insignificant role, which is supported by the CO results that reveal very weak Lewis acidity for coordinatively unsaturated Ba²⁺ sites. On the other hand, the broad and intensive band at 3009 cm⁻¹ indicates the predominance of the F \cdots H–CCl₃ interaction. This is the first time that in a fluoride material, the base is the dominating site in the acid–base pair couple. This result is supported by the ν_4 band, which gives rise to one band at 1219 cm⁻¹, meaning that the symmetry of CHCl₃ is the same as in the gas phase. Therefore, CHCl₃ reveals the dominating presence of Lewis basic sites in the acid–base pair for all BaF₂ samples.

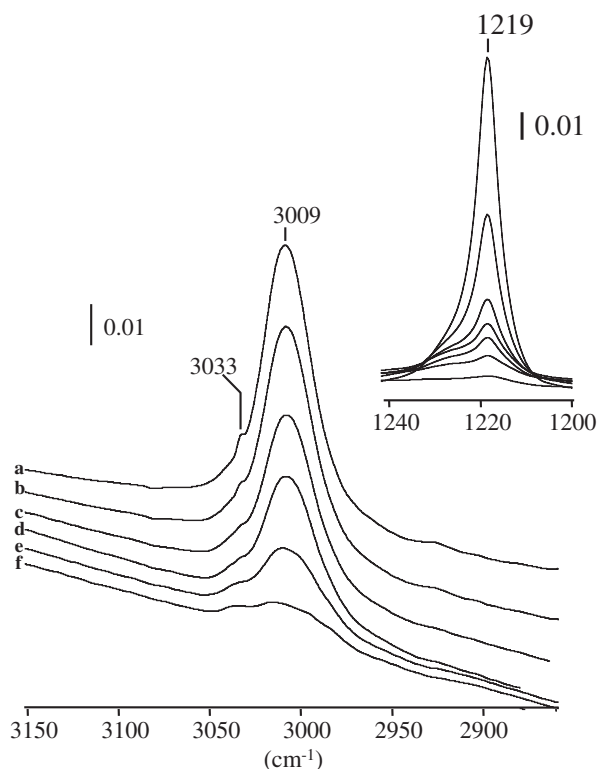


Fig. 5. IR spectra of $\text{BaCl}_{0.7}\text{F}_{1.3}$ outgassed at 473 K after adding 1 Torr (a) and 0.5 Torr (b) of CHCl_3 at equilibrium pressure and then outgassing (primary vacuum) for 1 min (c), 2 min (d), 5 min (e), and 10 min (f) (a–e are subtracted spectra from the background).

However, CHCl_3 is not a suitable probe molecule to elucidate the strength of Lewis basicity. For this purpose, pyrrole is a better probe molecule because it is able to form H-bonded species via the NH group with moderately basic surface centers [25]. Spectra recorded on $\text{BaCl}_{0.7}\text{F}_{1.3}$ after introducing 1 Torr of pyrrole at equilibrium pressure (Fig. 6a) show in the $\nu(\text{NH})$ range two bands at 3383 cm^{-1} and 3220 cm^{-1} . These two bands are red-shifted with respect to that of the gas phase ($\nu_{\text{gas}} = 3497\text{ cm}^{-1}$) indicating the presence of two different Lewis basic sites. The band at 3220 cm^{-1} is not sensitive to the outgassing procedure, whereas that at 3383 cm^{-1} is red shifted to 3300 cm^{-1} . This can be due to the fact that pyrrole adsorbed on the fluorine atom sites is affected by inductive interactions through the surface caused by pyrrole adsorption on neighboring sites. Therefore, removing adsorbed pyrrole could strengthen the other sites resulting in the observed red shift. This behavior suggests the presence of two different Lewis basic sites: the first being weak and the second with medium strength.

However, pyrrole adsorption that was found to be dissociative on the pure BaF_2 samples suggests the presence of medium/strong Lewis basic centers. For these cases, pyrrole is not any more meaningful due to the fact that it changes the acid–base surface properties of the sample. It can be concluded from the pyrrole adsorption on the different BaF_2 samples that $\text{BaCl}_{0.7}\text{F}_{1.3}$ possesses moderately strong Lewis basicity whereas the pure BaF_2 samples possess stronger basic sites.

3.2. Catalytic results

After an initial period of ca. 90 min, stable reaction rates of 3-chloro-1,1,1,3-tetrafluorobutane were observed for aluminum fluoride, calcium fluoride, strontium fluoride, and barium fluoride the latter handled in air (Fig. 7, Table 3). For aluminum fluoride

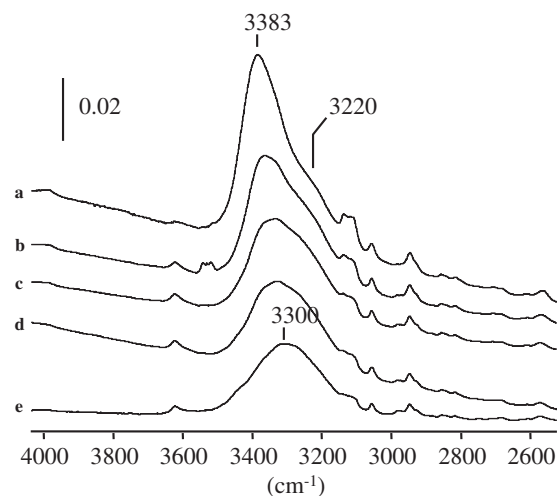


Fig. 6. IR spectra of $\text{BaCl}_{0.7}\text{F}_{1.3}$ outgassed at 473 K after adding 1 Torr of pyrrole at equilibrium pressure (a) and then outgassed under primary vacuum for 5 min (b) and 10 min (c) and under secondary vacuum for 5 min (d) and 10 min (e).

and barium fluoride handled in air, long-term measurements were performed: even after twenty hours, the reaction rate of 3-chloro-1,1,1,3-tetrafluorobutane was $0.06\text{ }\mu\text{mol s}^{-1}\text{ m}^{-2}$ (98% conversion) in the case of aluminum fluoride and $0.15\text{ }\mu\text{mol s}^{-1}\text{ m}^{-2}$ (92% conversion) for barium fluoride handled in air. The barium fluoride that had been handled under inert conditions displays a decrease in reactivity from $0.43\text{ }\mu\text{mol s}^{-1}\text{ m}^{-2}$ (90% conversion) after thirty minutes to $0.34\text{ }\mu\text{mol s}^{-1}\text{ m}^{-2}$ (72% conversion) after two hours. For magnesium fluoride, the reaction rate raises strongly during the first ninety minutes and approaches $0.30\text{ }\mu\text{mol s}^{-1}\text{ m}^{-2}$ (83% conversion) after two hours. The reaction rates found here are one to two magnitudes higher than these observed by Mishakov et al. for conversion of 1-chlorobutane over MgO at $200\text{ }^\circ\text{C}$ ($0.004\text{ }\mu\text{mol s}^{-1}\text{ m}^{-2}$) [10].

Despite the different catalytic activity and surface area of the both barium fluoride phases, they also differ in their degree of chlorination (Table 1). The barium fluoride handled in air exhibited significantly higher chlorine content than the inert handled one. Obviously, chlorination is faster when moisture is present. Probably, traces of water accelerate the chlorination of barium fluoride due to the formation of a thin liquid film of hydrogen chloride dissolved in water thus transforming the solid/gas into a solid/liquid reaction. $\text{BaCl}_{0.7}\text{F}_{1.3}$ formed this way is thermodynamically stable (Section 4) and the most active catalytic phase in the barium chloride fluoride system.

Aluminum fluoride is highly selective for the dehydrofluorination reaction of 3-chloro-1,1,1,3-tetrafluorobutane. The selectivity toward dehydrochlorination increases in the alkaline earth metal fluoride series with increasing atom number. Independent of its handling, barium fluoride is very selective for dehydrochlorination (Table 3).

In the case of calcium fluoride and strontium fluoride, which catalyze both, the dehydrochlorination as well as the dehydrofluorination of 3-chloro-1,1,1,3-tetrafluorobutane, the formation of 1,1,1,3-pentafluorobutane is observed. Very probably, it is formed by the reaction of *cis/trans*-1,1,1,3-tetrafluorobut-2-ene, formed via dehydrochlorination, with hydrogen fluoride also formed during the dehydrofluorination reaction. Hence, it is obviously a consecutive reaction product of the dehydrochlorination product with HF.

The desired product of the dehydrofluorination as well as the dehydrochlorination reaction of 3-chloro-1,1,1,3-tetrafluorobutane is that one with an end standing double bond (3-chloro-1,1,1-

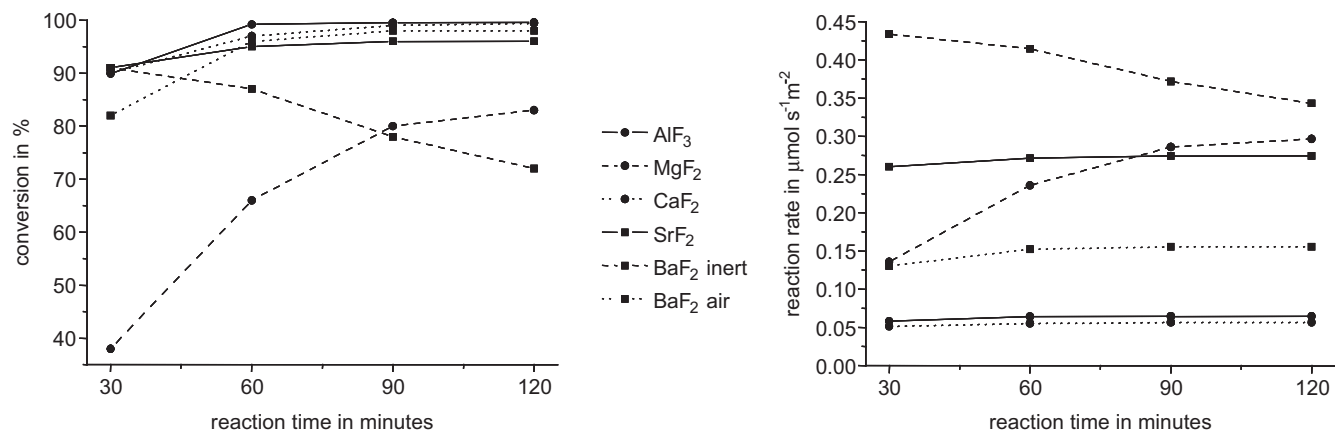


Fig. 7. Conversion of 3-chloro-1,1,1,3-tetrafluorobutane during 120 min with different catalysts and corresponding reaction rates.

Table 3

Catalytic data for the dehydrohalogenation of 3-chloro-1,1,1,3-tetrafluorobutane (C: conversion, S: selectivity).

Catalysts	C ₃ -chloro-1,1,1,3-tetrafluorobutane	Reaction rate ($\mu\text{mol s}^{-1} \text{m}^{-2}$)	S _{dehydrofluorination}	S _{dehydrochlorination}	S _{1,1,1,3,3-pentafluorobutane}
AlF ₃	>99%	(0.06)	1.0	0.0	0.0
MgF ₂	83%	0.30	0.9	0.1	0.0
CaF ₂	>99%	(0.06)	0.4	0.5	0.1
SrF ₂	96%	0.28	0.2	0.7	0.1
BaF ₂	72%	0.34	0.0	1.0	0.0
BaF ₂ air	98%	0.16	0.0	1.0	0.0

Table 4

Dependency of the desired product selectivity on contact time.

Catalyst	Contact time	C (%)	S _{3-chloro-1,1,1-trifluorobut-3-ene}	Catalyst	Contact time (s)	C (%)	S _{1,1,1,3-tetrafluorobut-3-ene}
AlF ₃	0.25	>99	0.78	BaF ₂ air	0.25	82	0.79
	0.50	>99	0.69		0.50	98	0.73

trifluorobut-3-ene, 1,1,1,3-tetrafluorobut-3-ene), which is kinetically preferred. With decreasing contact time, the selectivity toward these products increases, giving proof of the kinetic control (Table 4).

4. Discussion

Lewis acids are known to activate C–X bonds, which is the initial step of a dehydrohalogenation reaction. Thermodynamically C–F bond activation is less probable than C–Cl bond activation (490 kJ mol^{-1} vs. 340 kJ mol^{-1}) [26]. That is why, only very strong Lewis acids are expected to be active for dehydrofluorination in contrast to dehydrochlorination, which should be privileged for most of Lewis acidic catalysts.

As predicted, aluminum fluoride as a strong Lewis acid catalyzes the dehydrofluorination reaction. In contrast to our expectation, the dehydrochlorination reaction is completely suppressed. Basically, dehydrohalogenation should proceed via an activated surface complex of the respective haloalkane, which is initiated in the first step by the interaction of the alkane halogen atom with a coordinatively unsaturated surface site of the catalyst. The Lewis acidity of the non-saturated surface sites is expected to play a crucial role regarding activity (conversion) and selectivity (dehydrofluorination vs. dehydrochlorination). However, additional factors must play a role because thermodynamically dehydrochlorination should be privileged at all the Lewis acidic catalysts used, meaning C–Cl bond activation should be easier than C–F bond activation. Moreover, barium fluoride possesses only very weak Lewis acid

Table 5

Reaction enthalpies: Reaction of metal fluoride with HCl to metal chloride and HF.

	$\Delta_R H$ (kJ mol^{-1})
AlF ₃	263
MgF ₂	121
CaF ₂	71
SrF ₂	24
BaF ₂	–14

sites but catalyzes significantly and selectively the dehydrochlorination reaction. Thus, we believe that for the dehydrochlorination of 3-chloro-1,1,1,3-tetrafluorobutane, the Lewis acidity is not the determining factor. In contrast, by decreasing the Lewis acidity and increasing the Lewis basicity, the selectivity toward dehydrochlorination increases.

Thus, we believe that the affinity of the metal toward the respective halogen (strength of the metal–halogen bond) is a major decisive factor. In Table 5, the reaction enthalpies of chloride formation by reacting the respective metal fluoride with HCl are presented [27]. The formation of AlF₃ is significantly favored over the formation of AlCl₃. As a consequence, a selective interaction of the alkane F-atom with under coordinated aluminum surface sites of AlF₃ is expected in accord with the experimentally determined behavior. The situation changes within the alkaline earth metal series. With raising atom number, the thermodynamic tendency of fluoride formation drops down. In case of barium halogenide

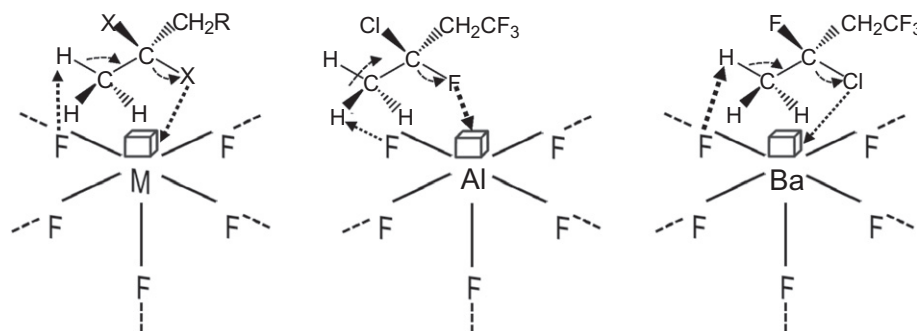


Fig. 8. Proposed catalytic mechanism for the dehydrofluorination and dehydrochlorination of 3-chloro-1,1,1,3-tetrafluorobutane.

formation, the reaction enthalpy is close to zero, that is, why no reaction pathway is favored and a barium chloride fluoride will be formed. In correspondence with this thermodynamic prediction, chlorination of BaF_2 resulting in the formation of $\text{BaCl}_{0.7}\text{F}_{1.3}$ – which is the catalytically active phase – has been observed.

Thus, the different dehydrohalogenation selectivities of aluminum fluoride and barium fluoride are an interrelation between the surface acid–base properties and the thermodynamic tendency of the under coordinated metal surface sites with the respective halogen atom. Going from aluminum fluoride to barium fluoride, the Lewis acidity decreases dramatically and, at the same time, the Lewis basicity increases. Moreover, also with this behavior, the predominance of the acid–base pair changes from acid site to basic site dominance. Last but not least, the affinity toward fluorine decreases from aluminum fluoride to barium fluoride, whereas the chlorine affinity increases. Therefore, a molecule like 3-chloro-1,1,1,3-tetrafluorobutane that can interact (like CHCl_3) with either a Lewis acid site or a base site changes in the predominant type of adsorption from AlF_3 to BaF_2 . Calcium fluoride and strontium fluoride catalyze both, the dehydrochlorination and the dehydrofluorination of 3-chloro-1,1,1,3-tetrafluorobutane. These two fluorides lay between aluminum fluoride and barium fluoride, meaning that in these samples neither the acid–base pairs are single dominant sites nor the affinity toward fluorine or chlorine is favored. Hence both reactions, dehydrochlorination and dehydrofluorination, might be rationalized as a consequence of the dominant hard–hard (Al–F) and soft–soft (Ba–Cl) interaction of the different types of metal fluoride catalysts used.

As a consequence, we would describe the catalytic mechanism as a simultaneous interaction of the halogen with the metal site and of a catalysts surface fluorine with a proton (Fig. 8). Thereby, the character of the metal site (affinity toward either to fluorine or chlorine, acid–base properties) defines the reaction pathway (dehydrochlorination or dehydrofluorination).

5. Conclusions

Aluminum fluoride and the alkaline earth metal fluorides prepared via the fluorolytic sol–gel synthesis are very selective dehydrohalogenation catalysts. It was found that dehydrofluorination is selectively catalyzed by strong Lewis acids (AlF_3 , MgF_2), while dehydrochlorination is completely suppressed. Interestingly enough, BaF_2 carries very weak acidic surface sites but catalyzes the dehydrochlorination selectively. The thermodynamic data show that the metal affinity toward chlorine or fluorine plays a decisive role. Reasonably, the reaction pathway is determined by the character of the metal site (affinity toward fluorine or chlorine, acid–base properties). Thus, we could successfully relate acid–base and thermodynamic properties of the catalysts with the catalytic behavior of the solid catalysts and with this giving mechanistic insight of

the reaction. Moreover, we successfully developed catalysts that are highly selective in the catalyzed dehydrofluorination or dehydrochlorination reaction for a substrate that can perform both reactions. We are now working to apply these catalysts on other substrates to extend this application. The final goal is to demonstrate that the sol–gel prepared nano-metal fluorides can be used as selective catalysts for the production of different haloalkenes from haloalkanes.

Acknowledgments

We thank S. Bäßler and A. Zehl (Humboldt-University, Berlin) for NH_3 -TPD and NH_3 -PAS analysis and chlorine content determination. K.T. is a stipendiate of the graduate school “Fluorine as key element” (GRK 1582) of Deutsche Forschungsgemeinschaft, DFG.

References

- [1] E. Kemnitz, U. Groß, S. Rüdiger, C.S. Shekar, *Angew. Chem.* 115 (2003) 4383; E. Kemnitz, U. Groß, S. Rüdiger, C.S. Shekar, *Angew. Chem. Int. Ed.* 42 (2003) 4251.
- [2] S. Rüdiger, U. Groß, E.J. Kemnitz, *Fluorine Chem.* 128 (2007) 353.
- [3] S. Wuttke, S.M. Coman, G. Scholz, H. Kirmse, A. Vimont, M. Daturi, S.L.M. Schroeder, E. Kemnitz, *Chem. Eur. J.* 14 (2008) 11488.
- [4] S. Wuttke, S.M. Coman, J. Kröhnert, F.C. Jentoft, E. Kemnitz, *Catal. Today* 152 (2010) 2.
- [5] S.M. Coman, S. Wuttke, A. Vimont, M. Daturi, E. Kemnitz, *Adv. Synth. Catal.* 350 (2008) 2517.
- [6] N. Candu, S. Wuttke, E. Kemnitz, S.M. Coman, V.I. Parvulescu, *Appl. Catal. A: Gen.* 391 (2011) 169.
- [7] A. Negoi, S. Wuttke, E. Kemnitz, D. Macovei, V.I. Parvulescu, C.M. Teodorescu, S.M. Coman, *Angew. Chem. Int. Ed.* 49 (2010) 8134.
- [8] S.M. Coman, V.I. Parvulescu, S. Wuttke, E. Kemnitz, *Chem. Commun.* (2009) 460.
- [9] S.M. Coman, V.I. Parvulescu, S. Wuttke, E. Kemnitz, *ChemCatChem* 2 (2010) 92.
- [10] (a) I.V. Mishakov, A.F. Bedilo, R.M. Richards, V.V. Chesnokov, A.M. Volodin, V.I. Zaikovskii, R.A. Buyanov, K.J. Klabunde, *J. Catal.* 206 (2002) 40; (b) V.B. Fenelenov, M.S. Mel'gunov, I.V. Mishakov, R.M. Richards, V.V. Chesnokov, A.M. Volodin, K.J. Klabunde, *J. Phys. Chem. B* 125 (2001) 3937.
- [11] C. Pistarino, E. Finocchio, M.A. Larrubia, B. Serra, S. Braggio, M. Baldi, *Ind. Eng. Chem. Res.* 40 (2001) 3262.
- [12] S. Kamiguchi, M. Watanabe, K. Kondo, M. Kodomari, T. Chihara, *J. Mol. Cat. A: Chem.* 203 (2003) 153.
- [13] U. Gross, S. Rüdiger, E. Kemnitz, *Solid State Sci.* 9 (2007) 838.
- [14] PDF-2 Database [Sets 1–51 plus 70–89], International Centre for Diffraction Data, 2001.
- [15] S. Ruediger, U. Groß, M. Feist, H.A. Prescott, S.C. Shekar, S.I. Troyanov, E. Kemnitz, *J. Mater. Chem.* 15 (2005) 588.
- [16] S. Wuttke, G. Scholz, S. Rüdiger, E. Kemnitz, *J. Mater. Chem.* 17 (2007) 4980.
- [17] S. Rüdiger, G. Eltanany, U. Groß, E. Kemnitz, *J. Sol–Gel Sci. Technol.* 41 (2007) 299.
- [18] S. Wuttke, A. Vimont, J.C. Lavalley, M. Daturi, E. Kemnitz, *J. Phys. Chem. C* 114 (2010) 5113.
- [19] K.I. Hadjiivanov, G.N. Vayssilov, *Adv. Catal.* 47 (2002) 307.
- [20] T. Krahl, A. Vimont, G. Eltanany, M. Daturi, E. Kemnitz, *J. Phys. Chem. C* 111 (2007) 18317.
- [21] P. Li, Y. Xiang, V.H. Grassian, S.C. Karsen, *J. Phys. Chem. B* 103 (1999) 5058.
- [22] V. Sadykov, R. Bunina, G. Alikina, A. Ivanova, D. Kochubei, B. Novgorodov, E. Paukshtis, V. Fenelonov, V. Zaikovskiy, T. Kuznetsova, S. Beloshapkin, V.

- Kolomichuk, E. Moroz, V. Matyshak, G. Konin, A. Rozovsky, J.R.H. Ross, J. Breen, *J. Catal.* 200 (2001) 117.
- [23] S. Huber, H. Knözinger, *J. Mol. Catal. A* 141 (1999) 117.
- [24] J.C. Lavalley, *Catal. Today* 27 (1996) 377.
- [25] C. Binet, A. Jadi, J. Lamotte, J.C. Lavalley, *J. Chem. Soc., Faraday Trans.* 92 (1996) 123.
- [26] NIST Chemistry WebBook – NIST Standard Reference Database Number 69, US Secretary of Commerce on behalf of the United States of America, 2008.
- [27] D.R. Lide, H.P.R. Frederikse, *CRC Handbook of Chemistry and Physics*, CRC Press, Inc., 1996.